This is the accepted manuscript made available via CHORUS. The article has been published as:

Transport coefficients in silicate melts from structural data via a structure-thermodynamics-dynamics relationship

Gaurav Goel, Daniel J. Lacks, and James A. Van Orman

Phys. Rev. E **84**, 051506 — Published 21 November 2011

DOI: 10.1103/PhysRevE.84.051506

Transport coefficients in silicate melts from structural data via a structure-thermodynamics-dynamics relationship

Gaurav Goel and Daniel J. Lacks*
Department of Chemical Engineering, Case Western Reserve University, Cleveland, OH 44106

James A. Van Orman†
Department of Geological Sciences, Case Western Reserve University, Cleveland, OH 44106

The viscosity and diffusivities of silicate melts under high pressure–high temperature conditions are difficult to obtain experimentally. Estimation and extrapolation of transport coefficients is further complicated by their extreme sensitivity to melt composition. Our molecular dynamics simulations show that, over a broad range of melt composition, temperature and pressure, the diffusivities correlate with the excess entropy; approximations to the latter can be obtained from the knowledge of the radial distribution function. Using this structure-thermodynamics-dynamics relationship, we show that transport properties of silicate melts can be estimated quantitatively using static structure factor data from experiments.

PACS numbers: Valid PACS appear here

A quantitative semi-empirical correlation between transport coefficients and excess entropy of simple atomic fluids was discovered by Rosenfeld in 1977 [1]. Since then, several computational and experimental studies have explored this transport-excess entropy correlation in complex fluids, e.g. water, ionic melts, model polymeric melts, etc ([2] and references within). Only a handful of these studies have looked at the effect of composition on the connection between transport properties and excess entropy of the mixture [2–4]. Silicate melts, where the viscosity at $T = 1000°\mathrm{C}$ can change by 10 orders of magnitude on changing silica content by about 30% [5], provide an excellent model system for further exploring the effect of composition on transport–excess entropy correlation.

In addition to providing an intriguing model system, the transport properties of silicate melts are relevant to formation and dynamics of the Earth's interior [6–8], and the nature of glass formed in metallurgical extractions [9, 10]. Estimation of viscosity and chemical diffusivities from laboratory or field data is made difficult by two unusual properties of silicate melts. Firstly, these melts can show an anomalous increase in the self-diffusion coefficients [11–13] or decrease in viscosity [14, 15] upon compression. Secondly, as noted above, the transport coefficients of silicate melts are extremely sensitive to the composition of the melt [5, 12, 16]. This complex behavior has been linked to the disruption of the polymerized tetrahedral framework of Si^{4+} (or Al^{3+}) cations by increasing pressure and/or increasing the concentration of network modifying oxides [12, 13]. However, a rigorous quantitative connection between the above mentioned structural changes and the transport coefficients of silicate melts, accounting for changes in composition, temperature, and pressure, is yet to be explored.

It is difficult to use existing techniques [17–20] for measuring self-diffusion coefficients and viscosity at geologically relevant high-temperature–high-pressure conditions. The static structure factor of silicate liquids, on the other hand, can be determined at much higher pressures and temperatures using laser heated diamond anvil cell techniques with synchrotron x-ray diffraction [21, 22] (It is difficult to apply laser heated diamond anvil cell techniques to determine transport coefficients because of the small size of the uniformly heated area.) Hence, a quantitative link between structure factor and transport coefficients will provide an indirect route to estimate the latter from static structure data for silicate melts.

Previously, the Adam-Gibbs relationship [23–25] has been used to map experimental data for melt transport coefficients on configurational entropy. The melt configurational entropy was shown to quantitatively track experimental trends in temperature variations of diffusivity and viscosity data at ambient pressure [26]. It was helpful in qualitatively explaining experimental results showing that the dynamics of polymerized liquids become faster with pressure (in a certain pressure range) and that of depolymerized liquids become slower with pressure [15, 24, 25, 27]. In this work we explore the applicability of excess entropy of the melt, s^{ex}, to describe transport properties of silicate melts. We will show that an approximation to excess entropy of the melt can be calculated from the structure factor of the melt, and hence, will allow us to quantitatively study both temperature and pressure variation of ion diffusivity in silicate melts.

Excess entropy of the melt is a fundamental thermodynamic quantity which captures the extent of interparticle correlations resulting from interparticle interactions. Rosenfeld [1, 28] has shown that transport properties of several simple fluids such as liquid metals, plasma, a model Lennard-Jones fluid, etc. scale quantitatively with

---

*Corresponding author; Electronic address: `djl15@case.edu`
†Corresponding author; Electronic address: `jav12@case.edu`

the excess entropy of the fluid according to,

$$L^* = A\exp(\alpha s^{\mathrm{ex}}) \quad (1)$$

Here L^* are transport coefficients nondimensionalized by appropriate combinations of macroscopic thermodynamic properties (e.g., density, temperature), and A and α are scaling parameters. The success of such a scaling relationship for predicting transport coefficients depends on state point independence of these scaling parameters, as observed in the above study for simple fluids. Since then, several experimental and simulation studies have shown that excess entropy also tracks the dynamics of more complex fluids such as water [29, 30], silica [31], nitrogen [32], and carbon dioxide [18], with scaling parameters invariant with temperature or both temperature and density.

To make a link to liquid static structure, we express s^{ex} by its multi-particle correlation expansion [33, 34], $s^{\mathrm{ex}} = \sum_{n=2}^{\infty} s_n$, where s_n is the entropy contribution from the n-particle spatial correlation function. The two-particle contribution, s_2, which is typically the dominant contribution to s^{ex} for a variety of fluids including ionic melts (e.g., SiO_2) [33, 35], is given as [33, 36]

$$s_2/k_{\mathrm{B}} = -\frac{\rho}{2}\sum_i\sum_j x_i x_j \int \{g_{ij}\ln g_{ij} - [g_{ij}-1]\}d\mathbf{r} \quad (2)$$

where, g_{ij} is the partial radial distribution functions (RDF) between the melt species. It has been shown that a scaling relationship similar to Eq. (1)- with s^{ex} replaced by s_2- tracks the self-diffusion data for fluids with contrasting RDFs to varying levels of universality (scaling parameters independent of species, density, and temperature for simple fluids [37] and independent of temperature and density or just temperature for complex network-forming fluids[38–40]). The choice of nondimensionalizing the transport coefficients with microscopic (atomic collision frequency and atomic diameter [37]) or macroscopic properties does not affect the universality of transport–s_2 correlation [40–43]. In this paper we use macroscopic properties for reducing the transport coefficients as these are more readily available in experiments. Further, the RDF data can be estimated from the inverse Fourier transform of static structure factor data, which can be obtained experimentally at high pressure and temperature. Thus, a correlation between s_2 and transport properties of silicate melts will be particularly useful for approximately estimating melt transport properties at the conditions of Earth's deep interior.

In this work we explore above correlation for pressure and temperature variations along the MgO-SiO_2 join. MgO and SiO_2 account for more than 80% of Earth's mantle by mass [44]. Additionally, melts along this join show large variations in structure (fully polymerized to depolymerized) as well as transport coefficients (more than 2 orders of magnitude change in self-diffusion coefficient of Si). Using molecular dynamics (MD) simulations, we first show that a strong correlation exists between self-diffusivity of network formers (Si, O) in silicate melts and melt excess entropy over a large parameter space spanning four compositions [$xSiO_2 - (1-x)MgO$, where x = 33%, 50%, 66%, and 100%], three temperatures [3000K, 4000K, and 5000K] and pressures between 0 (atmospheric) and 120 GPa. We then use the static structure factor data obtained from scattering experiments on silicate melts and the structure-thermodynamics-dynamics relationship obtained from MD simulations to estimate self-diffusivity of network formers in silicate melts. This is the first attempt to explore the effect of composition on the universality of self-diffusion–excess entropy correlation in silicate melts, and to use the structure factor data on silicate melts to predict self-diffusion coefficients.

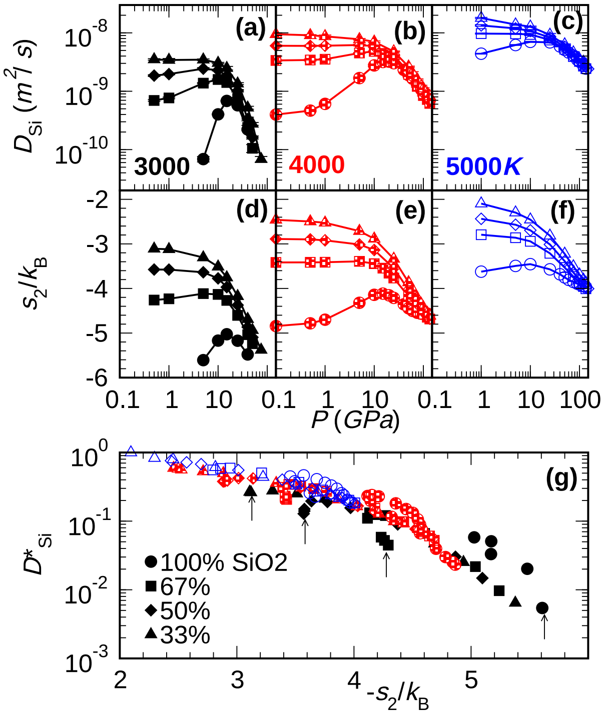

FIG. 1: (Color Online) Structure-thermodynamics-dynamics relationship in silicate melts. (a-c) Self-diffusivity of silicon D_{Si}, and, (d-f) two-body excess entropy s_2, in silicate melts plotted as a function of pressure at $3000K$, $4000K$, and, $5000K$. Lines are shown as a guide to eye. (c) Rosenfeld scaled silica self-diffusivity, $D^*{}_{\mathrm{Si}} = D_{\mathrm{Si}}\rho^{1/3}T^{-1/2}$, plotted as a function of (c) two-body excess entropy s_2 The data were calculated from molecular dynamics simulations for four compositions along the $SiO_2 - MgO$ join at $3000K$ (solid black), $4000K$ (shaded red), and $5000K$ (open blue), and pressures between 0–120 GPa. Arrows indicate the lowest density (pressure) at $T = 3000K$.

The simulations were carried out with the leap-frog Verlet algorithm in the NPT Gibbs ensemble of 2160 particles interacting via a modified [45] BKS [46] potential. A time step of $1fs$ was used in all the simulations. Temperature and pressure were controlled using the extended ensemble Nosé-Hoover thermostat ($\tau = 2$ps) and Parrinello-Rahman barostat ($\tau = 2$ps), respectively. Self-diffusivity of Si and O were calculated by fitting the long-time behavior of mean-squared displacement to the Einstein relation for diffusion $\left\langle \Delta\mathbf{r}^2 \right\rangle = 6Dt$, where $\left\langle \Delta\mathbf{r}^2 \right\rangle$ represents the mean-squared displacement, averaged over three Cartesian coordinates. Results are reported as averages over 5 independent $1ns$ trajectories recorded after each run was equilibrated for $1ns$. Because of slow relaxation, it was not possible to estimate equilibrium properties for SiO_2 at $3000K$ and $P \leq 1GPa$ within reasonable simulation time. A, further decrease in temperature will (approximately) exponentially slow down relaxation. Thus, we have restricted ourselves to temperatures above $3000K$. These simulations were done using the GROMACS [47, 48] package.

Figs. 1(a-c) shows the variation in self-diffusivity of Si with pressure along an isotherm in silicate melts. The self-diffusion coefficient of O (data not shown) follows the same trend as Si. For the most polymerized SiO_2 melt, D_{Si} first increases upon compression before decreasing. The depolymerized Mg_2SiO_4 melt, however, shows a decrease in D_{Si} with increasing compression in the entire pressure regime. These behaviors are analogous to those observed experimentally for silicate melts. For example, Shimizu and Kushiro reported that the O self-diffusion coefficient increased with pressure from 0.5 to 2 GPa in polymerized jadeite ($NaAlSi_2O_6$) melt and decreased with pressure from 1 to 1.7 GPa in depolymerized diopside ($MgCaSi_2O_6$) melt [12]. They interpreted the anomalous behavior of the jadeite melt to result from the collapse of the polymerized melt structure upon compression.

We show in Fig. 1(d-f) that the two-body excess entropy accounts for this anomalous behavior of D_{Si}. In accord with diffusivity, s_2 for the SiO_2 melt first increases with pressure indicating a decrease in the two-body correlations in the system. At higher pressures, s_2 decreases, mirroring the decrease in D_{Si}. Further, this non-monotonic pressure dependence of s_2 decreases with increasing MgO content, disappearing completely for Mg_2SiO_4. An analogous correspondence between viscosity and configurational entropy of silicate melts was obtained by taking into account the pressure dependence of the degree of polymerization of the melt [27]. Fig. 1(g) shows that there is a strong correlation between transport (D_{Si}) and structure (s_2) over a large parameter space spanning four different compositions (X) ranging from highly polymerized SiO_2 melt to a depolymerized Mg_2SiO_4 melt, a temperature (T) range spanning two orders of magnitude in diffusivity, and pressures (P) ranging from atmospheric to those characteristic of Earth's core-mantle boundary region. A similar relationship between viscosity and excess entropy has been shown to exist in experiments on water, nitrogen, and carbon dioxide [18, 30, 32].

This approximate collapse of transport–excess entropy data over a large range of values in the X–P–T parameter space greatly increases the usability of this correlation first observed in a SiO_2 melt [41]. It implies that X, P, and T play an analogous role in affecting transport processes in silicate melts. E.g., increasing one or more of structure modifier content, pressure, or temperature depolymerize the silicate melt (s_2 increases) resulting in a corresponding increase in D_{Si}. Secondly, it provides a route to estimate transport coefficients under conditions (e.g., extreme pressures) where direct experimental measurement is not possible. E.g., structure and transport measurements made in the $X - T$ plane at a fixed P can be used to obtain the scaling parameters in Eq. (1). The knowledge of these scaling parameters along with the structure factor data at the pressure of interest will provide an estimate for transport coefficients at that pressure. We elaborate on our approach below.

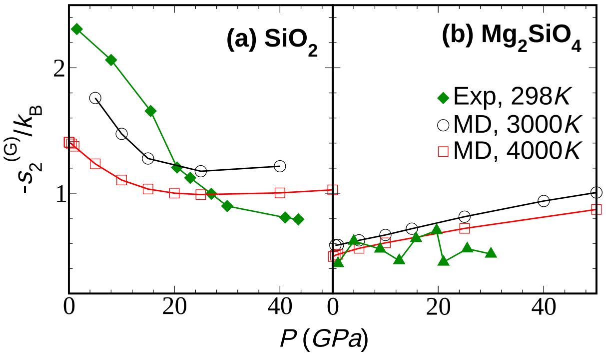

FIG. 2: (Color Online) Estimate for $s_2^{(\mathrm{G})}$ along an isotherm for silicate melts as determined from experimental static structure factor data $S(k)$. (a)&(b) $s_2^{(\mathrm{G})}$ calculated via Eq. (3) and plotted as a function of pressure for SiO_2 and Mg_2SiO_4 glasses at $298K$ (solid green diamond), respectively. The $S(k)$ data was obtained from Benmore et. al. [21, 53]. For comparison, MD data for SiO_2 and Mg_2SiO_4 melts at $3000K$ (open black circle) and $4000K$ (open red square) is also shown, respectively.

Note that although it is easy to obtain partial RDFs required to calculate s_2 (Eq. (2)) in simulations, it requires significantly more effort to obtain the partial RDFs in experiments. Each partial RDF would require the corresponding partial structure factor [49] which can only be obtained with a series of isotope substitution experiments [50]. In contrast, the total structure factor is obtained more straightforwardly using either inelastic neutron scattering [51] or high energy X-ray diffraction [21, 52]. The corresponding total RDF, $G(r)$, can be used to define an approximation to s_2 as follows,

$$s_2^{(\mathrm{G})}/k_{\mathrm{B}} = -\frac{\rho}{2}\int \{G(r)\ln G(r) - [G(r) - 1]\}d\mathbf{r} \qquad (3)$$

In Fig. 2, we compare MD estimates for $s_2^{(\mathrm{G})}$ of SiO_2 and Mg_2SiO_4 melts with corresponding $s_2^{(\mathrm{G})}$ as determined from the experimental structure factor data from Benmore et. al. [21, 53]. Our simulations capture the important structural variations in silicate melts. For the highly polymerized SiO_2 melt, $-s_2^{(G)}$ initially decreases on increasing pressure, but then changes only slowly on further increase in pressure; the effect of pressure becomes more significant as the temperature decreases, as indicated by the larger slope of the $s_2^{(G)}$–P curve at lower temperatures. For the depolymerized Mg_2SiO_4 melt, $s_2^{(G)}$ increases on increasing pressure. Our simulations quantitatively capture the large decrease in $-s_2^{(G)}$ on changing the composition from SiO_2 to Mg_2SiO_4.

Fig. 3(a) shows that $s_2^{(G)}/T$ tracks the Rosenfeld-scaled O self-diffusivity over the entire parameter space fairly accurately (although 100% SiO_2 data shows large deviations). Note that the total RDF $G(r)$, which is a weighted-average over partial RDFs [49], can be insensitive to details of individual RDFs. This results in a greater spread in the diffusivity–$s_2^{(G)}/T$ data compared with the diffusivity–s_2 data in Fig. 1(g). In fact, we needed to rescale the x-axis in Fig. 3(a) by k_BT to properly account for the effect of temperature on self-diffusivity.

We now test the usability of static structure factor data obtained using x-ray diffraction or neutron scattering experiments on silicate melts in predicting corresponding transport coefficients. In the range studied, an exponential fit of the form ${D^*}_O = A\exp\left[\frac{Bs_2^{(G)}}{k_BT}\right]$ describes the simulation data very well (Fig. 3(a)); except for the 100% SiO_2 melt at low temperatures which we discussed later. As shown in Fig. 3(a),(c), experimental data on diffusivity and structure for a $M^{2+}SiO_3$ ($M = Ca$ or Mg) melt at $2300K$ and ambient pressure shows a remarkable agreement with the fit to simulation data. This state point is well below the lowest temperature ($= 3000K$) in our simulations indicating that a correlation based on $s_2^{(G)}$ can be used to predict transport coefficients far away from the parameter space of observed correlation.

In fig. 3(c) we provide estimates for D_O in silicate melts with 33%–50% SiO_2 at $2300K$ and ambient pressure. To make these predictions we used the experimental structure factor data [22] for above melts to obtain $G(r)$ and, hence, $s_2^{(G)}$ according to eq. (3); these values were then plugged into the RHS of the ${D^*}_O$–$s_2^{(G)}$ correlation equation in Fig. 3 to obtain an estimate for D_O. Our estimate for D_O in a $MgSiO_3$ melt is in excellent agreement with the corresponding experimental value. The observed increase in D_O with decreasing SiO_2 content is in accord with the suggestion [22] that 42 to 38% SiO_2 melts are intermediate between two contrasting Si- and Mg-type liquid networks. The former is dominated by a continuous, sparse silicate network, and hence, has lower diffusivities. The latter is characterized by distorted magnesium percolation domains, and hence, has higher diffusivities. These predictions will need to be tested by measuring diffusivities in Mg-rich silicate melts.

In the end, we note certain limitations of the above approach. Fig. 3(b) shows that the fit to MD data overpredicts D_O in a silica melt at $2373K$ by several orders of magnitude. Also, the MD data for a SiO_2 melt at $3000K$ shows the maximum deviation from the fit. We believe these large deviations for melts rich in SiO_2 and at low temperatures result from a combination of two factors–(i) a different mechanism for transport in silica rich melts at low temperatures [13, 58] and (ii) use of an approximation to excess entropy based on total RDF. The upper bound on SiO_2 content and melt conditions (T and P) at which diffusivities will align with the fit in Fig. 3(a) is not known. Thus, the ${D^*}_O$–$s_2^{(G)}$ correlation presented here needs to be evaluated further at temperatures closer to the melting point of silicate melts ($\sim 2000K$). Additionally, alternative ways to calculate s^{ex} (instead of s_2 or $s_2^{(G)}$) at low temperatures can be explored, e.g., by using the thermochemical entropy data to determine s^{ex} analogous to calculation of configurational entropy. Earlier

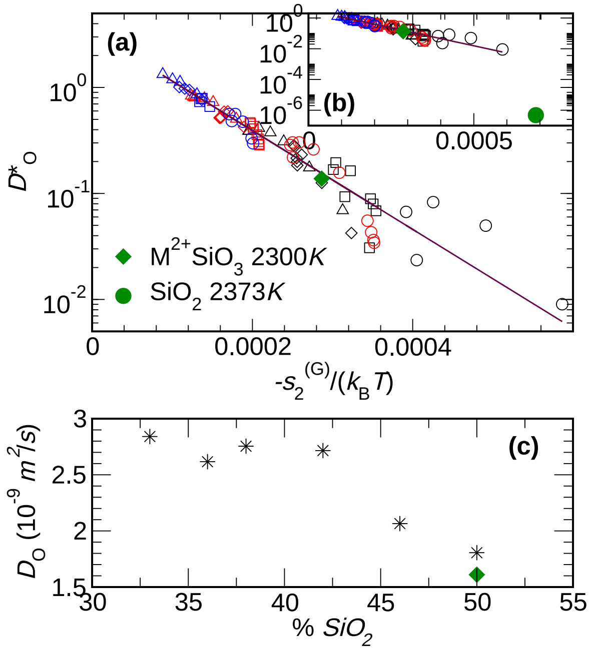

FIG. 3: (Color Online) Estimate for self-diffusivity of O in silicate melts. (a)&(b) A fit to the MD data (open symbols) for all four melt compositions in the temperature range $3000-5000K$ and pressure range $0-40GPa$, given by: ${D^*}_O = 3.36\exp[\frac{10736.3s_2^{(G)}K}{k_BT}]ms^{-1}K^{-1/2}$. Experimental data points at ambient pressure (filled symbols) are obtained as follows: self-diffusivity of O in a diopside ($CaOMgO(SiO_2)_2$) melt and Si in a silica melt obtained from the Arrhenius formulas in Refs. [54] and [55], respectively. The corresponding $s_2^{(G)}$ was determined from the structure factor data obtained using X-ray diffraction on $MgSiO_3$ at $2300K$ [22] ($MgSiO3$ and $CaOMgO(SiO_2)_2$ have the same network modifying oxide content ($\sum CaO+MgO = 50\%$)) and SiO_2 at $2373K$ [56]. An estimate for densities of silicate melts at above temperatures was obtained form the partial molar volumes of MgO and SiO_2 given in Ref. [57]. (c) Our prediction (stars) for compositional dependence of D_O in magnesium silicates at $2300K$ and ambient pressure.

work on supercooled liquids suggests that an equation of the form given by (1) might still be valid in this regime, although with different scaling variables [59–62].

To summarize the excellent collapse of self-diffusion–s_2 data collected over a broad range in the composition-temperature-pressure phase space provides empirical evidence that all three variables affect the transport processes in silicate melts in a similar manner. It will be interesting to explore if these correlations similarity extend to other transport processes in silicate melts, e.g. isotopic fractionation in silicate melts by thermal diffusion [63].

This material is based upon work supported by the National Science Foundation under Grant Nos. 0944238 and 1019749. We would like to thank Drs. J. L. Yarger and M. C. Wilding for providing us the X-ray diffraction structure factor data for silicate melts. We would like to thank the Ohio Supercomputing Center for providing computational resources for this study.

[1] Y. Rosenfeld, Phys. Rev. A **15**, 2545 (1977).
[2] W. P. Krekelberg, M. J. Pond, G. Goel, V. K. Shen, J. R. Errington, and T. M. Truskett, Phys. Rev. E **80**, 061205 (2009).
[3] A. Samanta, Sk.Musharaf Ali, and S. K. Ghosh, Phys. Rev. Lett. **87**, 245901 (2001).
[4] M. J. Pond, W. P. Krekelberg, V. K. Shen, J. R. Errington, and T. M. Truskett, J. Chem. Phys. **131**, 161101 (2009).
[5] D. Giordano and D. B. Dingwell, Earth Planet. Sci. Lett. **208**, 337 (2003).
[6] Y. Abe, Phys. Earth Planet. In. **100**, 27 (1997).
[7] S. ichiro Karato and V. R. Murthy, Phys. Earth Planet. In. **100**, 61 (1997).
[8] D. C. Rubie, H. J. Melosh, J. E. Reid, C. Liebske, and K. Righter, Earth Planet. Sci. Lett. **205**, 239 (2003).
[9] L. L. Hench, J Am. Ceram. Soc. **74**, 1487 (1991).
[10] H. Kim, F. Miyaji, T. Kokubo, C. Ohtsuki, and T. Nakamura, J Am. Ceram. Soc. **78**, 2405 (1995).
[11] C. A. Angell, P. A. Cheeseman, and S. Tamadon, Science **218**, 885 (1982).
[12] N. Shimizu and I. Kushiro, Geochim. Cosmochim. Acta **48**, 1295 (1984).
[13] B. T. Poe, P. F. McMillan, D. C. Rubie, S. Chakraborty, J. Yarger, and J. Diefenbacher, Science **276**, 1245 (1997).
[14] A. Suzuki, E. Ohtani, K. Funakoshi, H. Terasaki, and T. Kubo, Phys. Chem. Miner. **29**, 159 (2002).
[15] H. Behrens and F. Schulze, Am. Mineral. **88**, 1351 (2003).
[16] Y. Liang, F. M. Richter, A. M. Davis, and E. B. Watson, Geochimica et Cosmochimica Acta **60**, 4353 (1996).
[17] D. Tinker, C. E. Lesher, G. M. Baxter, T. Uchida, and Y. Wang, Am. Mineral. **89**, 1701 (2004).
[18] E. H. Abramson, Phys. Rev. E **80**, 021201 (2009).
[19] J. E. Reid, B. T. Poe, D. C. Rubie, N. Zotov, and M. Wiedenbeck, Chem. Geol. **174**, 77 (2001).
[20] J. A. Van Orman, Y. Fei, E. H. Hauri, and J. Wang, Geophys. Res. Lett. **30**, 1056 (2003).
[21] C. J. Benmore, E. Soignard, S. A. Amin, M. Guthrie, S. D. Shastri, P. L. Lee, and J. L. Yarger, Physical Review B **81**, 054105 (2010).
[22] M. C. Wilding, C. J. Benmore, and J. K. R. Weber, Europhys. Lett. **89**, 26005 (2010).
[23] G. Adam and J. H. Gibbs, J. Chem. Phys. **43**, 139 (1965).
[24] J. G. Bryce, F. J. Spera, and D. J. Stein, Am. Mineral. **84**, 345 (1999).
[25] D. R. Neuville, Chem. Geol. **229**, 28 (2006).
[26] Y. Bottinga and P. Richet, Chem. Geo. **128**, 129 (1995).
[27] Y. Bottinga and P. Richet, Geochim. Cosmochim. Acta **59**, 2725 (1995).
[28] Y. Rosenfeld, J. Phys.-Condens. Mat. **11**, 5415 (1999).
[29] J. Mittal, J. R. Errington, and T. M. Truskett, J. Chem. Phys. **125**, 076102 (2006).
[30] E. H. Abramson, Phys. Rev. E **76**, 051203 (2007).
[31] M. Agarwal, A. Ganguly, and C. Chakravarty, J. Phys. Chem. B **113**, 15284 (2009).
[32] E. H. Abramson and H. West-Foyle, Phys. Rev. E **77**, 041202 (2008).
[33] A. Baranyai and D. J. Evans, Phys. Rev. A **40**, 3817 (1989).
[34] R. E. Nettleton and M. S. Green, J. Chem. Phys. **29**, 1365 (1958).
[35] R. Sharma, M. Agarwal, and C. Chakravarty, Mol. Phys. **106**, 1925 (2008).
[36] R. D. Mountain and H. J. Raveché, J. Chem. Phys. **55**, 2250 (1971).
[37] M. Dzugutov, Nature **381**, 137 (1996).
[38] J. Mittal, J. Errington, and T. M. Truskett, J. Phys. Chem. B **110**, 18147 (2006).
[39] J. Mittal, J. Errington, and T. M. Truskett, J. Phys. Chem. B **111**, 5531 (2007).
[40] M. Agarwal and C. Chakravarty, Phys. Rev. E **79**, 030202 (2009).
[41] R. Sharma, S. N. Chakraborty, and C. Chakravarty, J. Chem. Phys. **125**, 204501 (2006).
[42] M. E. Johnson and T. Head-Gordon, J. Chem. Phys. **130**, 214510 (2009).
[43] R. Chopra, T. M. Truskett, and J. R. Errington, J. Phys. Chem. B **114**, 10558 (2010).
[44] W. F. McDonough and S. S. Sun, Chem. Geo. **120**, 223 (1995).
[45] D. J. Lacks, D. B. Rear, and J. A. Van Orman, Geochim. Cosmochim. Acta **71**, 1312 (2007).
[46] B. W. H. van Beest, G. J. Kramer, and R. A. van Santen, Phys. Rev. Lett. **64**, 1955 (1990).
[47] E. Lindahl, B. Hess, and D. van der Spoel, J. Mol. Mod. **7**, 306 (2001).
[48] H. J. C. Berendsen, D. van der Spoel, and R. van Drunen, Comp. Phys. Comm. **91**, 43 (1995).
[49] T. E. Faber and J. M. Ziman, Philos. Mag. **11**, 153 (1965).
[50] P. H. Gaskell, M. C. Eckersley, A. C. Barnes, and P. Chieux, Nature **350**, 675 (1991).
[51] F. Kargl and A. Meyer, Chem. Geol. **213**, 165 (2004).
[52] M. C. Wilding, C. J. Benmore, J. A. Tangeman, and S. Sampath, Chem. Geol. **213**, 281 (2004).
[53] J. L. Yarger, private Communication.
[54] T. Dunn, Geochim. Cosmochim. Acta **46**, 2293 (1982).
[55] G. Brebec, R. Seguin, C. Sella, J. Bevenot, and J. Martin,

Acta Metallurgica **28**, 327 (1980).

[56] Q. Mei, C. J. Benmore, and J. K. R. Weber, Phys. Rev. Lett. **98**, 057802 (2007).

[57] P. Courtial and D. B. Dingwell, Am. Mineral. **84**, 465 (1999).

[58] P. G. Debenedetti, *Metastable liquids: concepts and principles* (Princeton University Press, 1996).

[59] W. P. Krekelberg, J. Mittal, V. Ganesan, and T. M. Truskett, J. Chem. Phys. **127**, 044502 (2007).

[60] J. Mittal, J. Errington, and T. M. Truskett, J. Phys. Chem. B **111**, 10054 (2007).

[61] C. Kaur, U. Harbola, and S. P. Das, J. Chem. Phys. **123**, 034501 (2005).

[62] M. Agarwal, M. Singh, B. S. Jabes, and C. Chakravarty, J. Chem. Phys. **134**, 014502 (2011).

[63] F. Huang, P. Chakraborty, C. C. Lundstrom, C. Holmden, J. J. G. Glessner, S. W. Kieffer, and C. E. Lesher, Nature **464**, 396 (2010).